

## **OPTIMIZING BUILDING DESIGNS USING A ROBUSTNESS INDICATOR WITH RESPECT TO USER BEHAVIOR**

P. Hoes<sup>1,2</sup>, M. Trcka<sup>2</sup>, J.L.M. Hensen<sup>2</sup> and B. Hoekstra Bonnema<sup>3</sup>

<sup>1</sup>Materials innovation institute (M2i), The Netherlands

<sup>2</sup>Technische Universiteit Eindhoven (TU/e), The Netherlands

<sup>3</sup>Tata Steel Construction Centre, The Netherlands

### **ABSTRACT**

Multi-objective optimization algorithms are used in the building design process to find optimal solutions for design problems. Typically, these algorithms provide the decision maker with a Pareto front containing trade-off solutions. Since these solutions are equally good, the decision maker needs a method to select the most appropriate solution. In this paper, we propose a selection method that ranks the Pareto solutions according to their performance robustness. This allows the decision maker to select the most robust design solution. The proposed method is applied to an optimization problem of a building case study. The building performance robustness of this building is assessed for uncertainties in user behavior, since, for many buildings, that is a parameter with a high uncertainty and a high influence on the building performance. Our study shows that the proposed method provides the decision maker with useful information for the decision making process.

### **INTRODUCTION**

During the last decade, there has been an increasing interest in using optimization algorithms in the building design process, e.g., (Emmerich et al., 2008, Hopfe, 2009). These algorithms are used to find design solutions with the best possible building performance. In many cases, the optimization problem consists of two (or more) conflicting objectives, e.g. minimizing the energy demand while maximizing thermal comfort. It is impossible to find one best design solution (or design alternative) for these so-called multi-objective optimization problems (Deb et al. 2002, Coello Coello, 2005). Instead, a set of 'trade-offs' or good compromise solutions between the objectives are found. All solutions of this set are equally good, and the solutions are all Pareto optimal (meaning that an increase of one objective would simultaneously lead to a decrease of the other objective). The decision

maker should select one of these Pareto optimal solutions. Typically, multi-criteria decision making (MCDM) methods are used to support the decision maker in this selection process, e.g., using utility functions. In this paper, we propose a method based on the performance robustness of the Pareto solutions.

We define performance robustness as the ability of a building to handle changes (or disturbances) in the building's environment and maintain the required performance, based on Ferguson et al. (2007). Therefore, it is important to take performance robustness into account during the design process (Leyten and Kurvers, 2006). The proposed MCDM method ranks the Pareto solutions according to their performance robustness. This allows the decision maker to select the most robust solution.

In the present study, the performance robustness of the design alternatives is assessed by investigating the sensitivity of the building performance to changes in the behavior of the building users. We focus on user behavior because recent studies show that building performance can be highly sensitive to user behavior (Macdonald, 2002, Hoes et al., 2009). Moreover, according to the literature, the prediction of user behavior shows a high uncertainty (Andersen, 2009, Macdonald, 2002). This high sensitivity and high uncertainty makes user behavior an important parameter to take into account when assessing performance robustness.

The proposed MCDM method is applied to an optimization problem of a building case study. We show how it is implemented in the optimization run, and how this implementation can be used to optimize the building design under uncertainty of user behavior.

### **ROBUSTNESS INDICATOR**

The performance robustness of each Pareto solution is assessed by investigating the sensitivity of the building performance to changes in the building's

environment. These changes are of an uncertain (aleatory) nature and are represented by uncertainty scenarios (described in more detail in the next section). The uncertainty scenarios are used to simulate the building performance of each Pareto solution. The influence of the uncertainty scenarios on the building performance indicators is assessed by investigating the variation of the performance indicators. The variation is defined using the relative standard deviation (RSD):

$$RSD = \frac{SD}{\bar{x}} \quad (1)$$

with  $\bar{x}$  the estimated mean of the performance indicator with  $m$  samples (uncertainty scenarios) of the performance indicator ( $x$ ):

$$\bar{x} = \frac{1}{m} \sum_{i=1}^m x_i \quad (2)$$

and  $SD$  the estimated standard deviation of the performance indicator with  $m$  samples (uncertainty scenarios) of the performance indicator ( $x$ ):

$$SD = \sqrt{\frac{1}{m-1} \sum_{i=1}^m (x_i - \bar{x})^2} \quad (3)$$

The RSD is a dimensionless quantity of the variation, so it can be used to compare performance indicators with different units. In terms of robustness, we seek the smallest RSD in all performance indicators.

### Objectives vector

In this paper, the multi-objective optimization is based on two objectives (the building performance indicators, which are described in the next section). For every Pareto solution, we use the RSDs of both objectives to describe a vector  $\mathbf{v} = (x, y) = (RSD_{\text{objective1}}, RSD_{\text{objective2}})$  (Figure 1). From here on, we refer to this vector as the *objectives vector*. The length of the *objectives vector* is a quantified indicator for the robustness of the solution: the smaller the *objectives vector length*, the more robust the solution. Therefore, the length can be used to rank the Pareto solutions according to their robustness.

### Comparing solutions with the same objectives vector length

The angle of the *objectives vector* can be used to support the decision making process between solutions with the same *objectives vector length*. This angle gives information about the balance of the robustness between both objectives. An angle of 45° indicates that the RSDs of the two objectives are

the same; this is regarded as balanced robustness (Figure 1). An angle not equal to 45° indicates that one of the RSDs is larger than the other; this is regarded as unbalanced robustness (Figure 1). We define the *robustness balance* ( $\alpha$ ) as:

$$\alpha = \beta - 45^\circ \quad (4)$$

with  $\beta$  the *objectives vector angle*:

$$\tan \beta = \frac{RSD_2}{RSD_1} \quad (5)$$

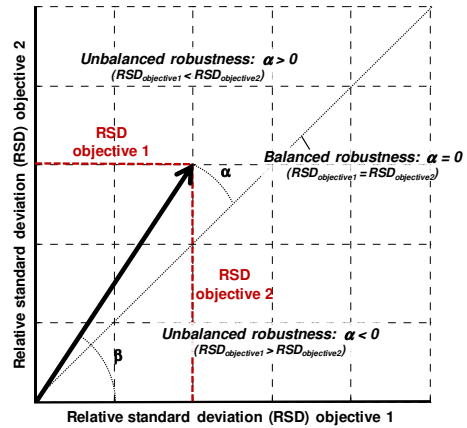


Figure 1: Example of an objectives vector. The length of the objectives vector is an indicator of the solution's performance robustness. The angle of the objectives vector gives information about the balance of the robustness between both objectives.

### Selection criterion based on $\alpha$

The decision maker (DM) can use  $\alpha$  as a secondary selection criterion when he has to choose between solutions with the same *objectives vector length*. For example, if the DM requires a solution with balanced robustness, then he should select the solution with  $\alpha$  closest to 0°. Or, if the DM is interested in a solution with one of the objectives being more robust than the other, then he should define a selection criterion of unbalanced robustness, e.g.,  $\alpha < 0^\circ$  or  $\alpha > 0^\circ$ .

### Selection criterion based on preferred $\alpha$

The DM can also decide between solutions by regarding the impact of the RSD on the objective values in the objective space. For example, the DM wants to minimize both objectives and he is confronted with two Pareto solutions which are positioned exactly at the same position on the upper-left side of a convex Pareto front (this position is marked with number 1 in Figure 2): the first solution shows  $\alpha = 0^\circ$  and the second solution  $\alpha < 0^\circ$ . Because of the position, these solutions show low values for objective 1 and high values for objective 2 compared to the maximum objective values. Regarding objective 2, this means that when the

solution shifts to the right on the Pareto front, the SD will get smaller with the same RSD (compare position 1 with position 2 and 3 in Figure 2). If we assume that the DM is searching for a solution with small SD's, then he will prefer the smallest available  $RSD_{objective2}$  for a solution at position 1. While he allows a larger  $RSD_{objective2}$  at position 3. Following the same reasoning, the DM would prefer the smallest available  $RSD_{objective1}$  for a solution at position 3. In the example with the two solutions at the same position, the DM should prefer the solution with  $RSD_{objective2} < RSD_{objective1}$ , thus the second solution with  $\alpha < 0^\circ$ .

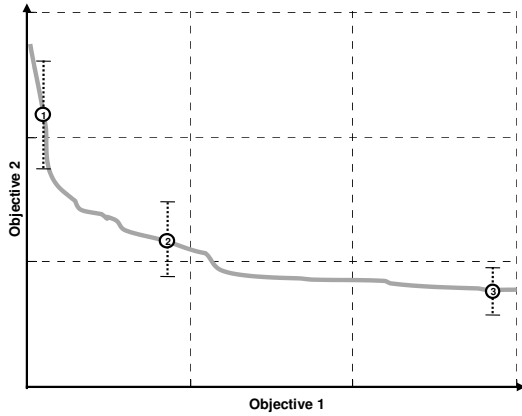


Figure 2: Example of how the position of a solution on the Pareto front influences the performance robustness. A solution is plotted at three different positions. The bars show the solution's performance uncertainty (SD) for objective 2. Position 3 shows the most robust performance (i.e. the smallest SD).

Generally, every solution has a *preferred  $\alpha$*  which depends on the position of the solution on the Pareto front. Since we assume that both objectives are equally important to the DM, we can calculate the *preferred  $\alpha$*  by first normalizing the objective values as follows:

$$objective_j^* = \frac{objective_j}{max_j} \quad (6)$$

and:

$$SD_j^* = \frac{SD_j}{max_j} = \frac{RSD_j \cdot objective_j}{max_j} \quad (7)$$

with  $j$  is 1 or 2, and  $max$  is the maximum value of the objective on the Pareto front. We want to minimize both  $SD^*$ 's. However, since we can only change  $\alpha$  to influence the  $SD^*$ 's, it is impossible to minimizing both  $SD^*$ 's at the same (e.g. when  $SD_1^*$  increases,  $SD_2^*$  will decrease). Thus, the trade-off is to find the  $\alpha$  when the  $SD^*$ 's are equal:

$$SD_1^* = SD_2^* \quad (8)$$

From (7) this can be written as:

$$\frac{RSD_1 \cdot objective_1}{max_1} = \frac{RSD_2 \cdot objective_2}{max_2} \quad (9)$$

Which can be written as:

$$\frac{RSD_2}{RSD_1} = \frac{objective_1 \cdot max_2}{objective_2 \cdot max_1} \quad (10)$$

From (6), it follows that:

$$\frac{RSD_2}{RSD_1} = \frac{objective_1^*}{objective_2^*} \quad (11)$$

Using (4) and (5), we calculate the *preferred  $\alpha$*  as:

$$preferred \alpha = \arctan\left(\frac{objective_1^*}{objective_2^*}\right) - 45^\circ \quad (12)$$

when  $objective_2^* = 0$ , then the preferred  $\alpha = 45^\circ$ .

Figure 3 shows the normalized Pareto front of Figure 2. The *preferred  $\alpha$* 's are shown for the three positions.

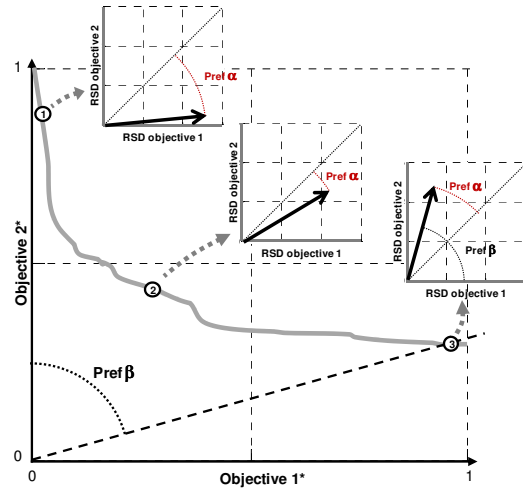


Figure 3: Normalized Pareto front with three solution positions and their preferred  $\alpha$ 's. The preferred  $\beta$  for position 3 is also shown.

The solution with an  $\alpha$  closest to the *preferred  $\alpha$*  is regarded as the preferred solution. The DM might want to define constraints on the RSDs to prevent them from becoming too large (e.g. maximum  $RSD_{objective1}$  is 1.5).

## CASE STUDY

The Pareto solution selection methodology is applied to a design optimization problem of a building. The problem consists of finding the building's optimal window size in combination with the optimal quantity of thermal mass for the spring season<sup>1</sup>. In this case study, we are using the Non-dominated Sorting Genetic Algorithm II (NSGA-II) (Deb et al., 2002) to find the Pareto solutions. NSGA-II is a well-known multi-objective optimization algorithm and has already been used in building performance simulation (Emmerich et al., 2008, Hopfe, 2009).

<sup>1</sup> This paper is related to the HATS project (Hoes et al., 2011) in which we search for the optimal thermal storage capacity of a building during the year (e.g. per day, per month or per season).

## Building case study

The building case study is defined in cooperation with Tata Steel Construction Centre. The building is based on the residential houses of the Zonne-entree project (Tata Steel Star-Frame and Courage Architecten bna) in Apeldoorn (the Netherlands). The building is modelled and simulated with the dynamic whole-building performance simulation tool ESP-r (Clarke, 2001) using a weather file of the Dutch climate. The case study consists of five zones: zone A (south orientated) and B (north orientated) on the ground floor and zone C, D (south orientated) and E (north orientated) on the first floor (Figure 4). The building is heated with an all-air system. The air temperature heating set points are set to 21°C when the room is occupied and 14°C when the room is not occupied; more details are given in Table 1 and Figure 4. The south façade is provided with an external shading device (horizontal venetian blinds). During winter months, the blinds are retracted making use of solar gains. During summer months, the blinds are lowered with slats set to 0 degrees (horizontal position). The slats are set to 80 degrees when the solar irradiance on the façade is higher than 300 W/m<sup>2</sup>. Two people are using the building during evenings (18h to 24h) and nights (24h to 8h).

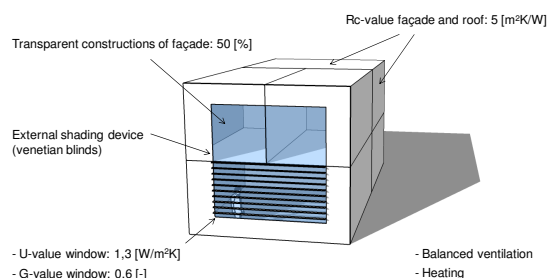


Figure 4: Case study based on Zonne-entree Apeldoorn, facing the south façade.

Table 1: Input parameters of case study Zonne-entree Apeldoorn.

|    | Input parameters                              | Value   | Unit                                   |
|----|---|---------|--|
| 1. | Occupancy                                     | evening | [-]                                    |
| 2. | Internal heat gains                           | 4.0     | [W/m <sup>2</sup> ]                    |
| 3. | Window type (U-value)                         | 1.3     | [W/m <sup>2</sup> K]                   |
| 4. | Thermal resistance façades                    | 5       | [m <sup>2</sup> K/W]                   |
| 5. | Infiltration ( $q_{infiltration,qv10,spec}$ ) | 0.08    | [dm <sup>3</sup> /s p.m <sup>2</sup> ] |
| 6. | Heating set point occupied)                   | 21      | [°C]                                   |
| 7. | Heating set point unoccupied                  | 14      | [°C]                                   |
| 8. | Ventilation                                   | 1.0     | [dm <sup>3</sup> /s p.m <sup>2</sup> ] |

## Design variables

The optimization algorithm is allowed to change the window size to 25%, 50% or 90% of the total north and south façades. The algorithm changes the thermal mass of the building by altering the density of the materials that are in contact with the indoor environment. The required density is calculated

using the effective thermal mass method (in Dutch the Specifiek Werkzame Massa or SWM). The effective thermal mass is a simplified quantification of the thermal mass. It is defined as the mass of the thermal-active layers of the surfaces in a room divided by the total area of the surfaces; e.g. low thermal mass is 5 kg/m<sup>2</sup> (lightweight floors and walls), medium thermal mass is 50 kg/m<sup>2</sup> (concrete floors, lightweight walls) and high thermal mass is 100 kg/m<sup>2</sup> (heavy concrete floors and walls). The optimization algorithm is allowed to change thermal mass per zone between 5 and 100 kg/m<sup>2</sup>.

## Performance indicators

The performance of the building is assessed using two performance indicators: the heating energy demand and the summed weighted over- and underheating hours. The heating energy demand is calculated in kWh/m<sup>2</sup> for the simulated spring period. The over- and underheating hours (WOH-Σ) are weighted with a factor that is a function of the PPD (Hoes et al., 2010).

To ensure a certain level of thermal comfort, a constraint is set on the number of WOH-Σ; the maximum allowed number of WOH-Σ is 200 hours. When solutions are assessed taking into account uncertainties, the same constraint is put on the *mean* WOH-Σ of the uncertainty scenarios. This is regarded as a loose constraint since it is accepted that in some cases the solutions exceed the limit. If we do not accepted that the solutions exceed the limit, we can also define a stricter constraint by applying a constraint on the maximum value of each uncertainty scenario.

## Uncertainty scenarios

As mentioned in the Introduction, the uncertainty scenarios are based on variations in user behavior (or lifestyles). In building performance simulation, user behavior is modelled with predefined diversity profiles or with more advanced stochastic and activity based models (Bourgeois, 2005, Haldi, 2009, Hoes et al., 2009, Tabak, 2010). Thus, we discern two approaches to generate the user behavior scenarios:

A simplified approach: user scenarios are defined based on combinations of predefined values for the input parameters that describe user behavior, e.g., heating set points, internal heat gains and ventilation rates.

An advanced approach: user scenarios are generated with stochastic user behavior models or activity based models.

In this paper we use the simplified approach. The values of the input parameters used to generate uncertainty variants are shown in Table 2.

Table 2: Parameters of uncertainty variants.

|  | Low | Mid | High |
|--|-----|-----|------|
| Heating set point occupied [°C]                    | 20  | 21  | 22   |
| Heating set point unoccupied [°C]:                 | 13  | 14  | 15   |
| Internal heat gains [W/m <sup>2</sup> ]            | 2   | 4   | 6    |
| Ventilation [dm <sup>3</sup> /s p.m <sup>2</sup> ] | 0.8 | 1.0 | 1.2  |

## PERFORMANCE ROBUSTNESS OF PARETO SOLUTIONS

Figure 5 shows the optimization result for the spring period. The building design is optimized for one user scenario (the ‘middle’ values of Table 2), thus without uncertainty scenarios. Shown are the Pareto solutions found after 100 generations with a population size of 20. The optimization algorithm was able to find 166 Pareto solutions. The DM should choose one of the solutions. For example, he can choose the solution that shows the lowest energy demand and still meets the WOH- $\Sigma$  constraint (the solution on the lower-right of the Pareto front). However, by doing this, the DM actually transforms the problem into a single objective optimization problem, and thus, he disregards many interesting design solutions (i.e. the other Pareto solutions).

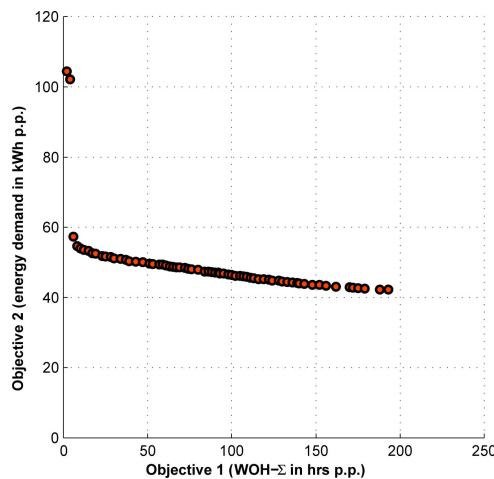


Figure 5: Result of the optimization for spring period. The dots represent the Pareto solutions.

To provide the DM with more information about the Pareto solutions, we define the performance robustness of each solution using the robustness indicator. To do this, we defined 9 uncertainty scenarios based on the ‘low’ and ‘high’ values of the uncertainty parameters in Table 2. The performance of all Pareto solutions is simulated with these uncertainty scenarios. The results for an arbitrarily chosen solution are shown in Figure 6. The figure shows the values of the normalized performance

indicator for the uncertainty scenarios. The *objectives vector* of this solution is plotted in the same figure; the *objectives vector length* ( $R$ ) is 2.04 and the *robustness balance* ( $\alpha$ ) is 12.46°.

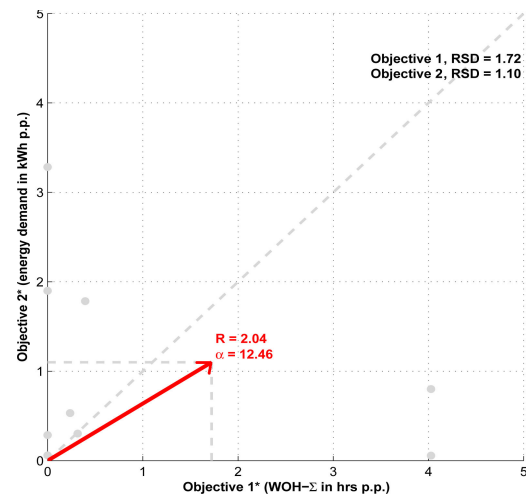


Figure 6: Normalized performance indicators of a solution for spring period. The *objectives vector* is plotted in the same graph ( $R = 2.04$  and  $\alpha = 12.46^\circ$ ).

In Figure 7, the *objectives vectors* of all Pareto solutions are presented in a scatter plot. The mean values of all solutions are plotted. The dot size in the scatter plot indicates the robustness (the smaller, the more robust); the dot color indicates the  $\alpha$  according to the color bar on the side of the graph. The three solutions with the smallest  $R$  and the solution with the largest  $R$  are marked with numbers (ascending from small to large) next to the dots. For these solutions, the size of  $R$  compared to the smallest  $R$  is shown between brackets. The performance indicator values of these solutions are presented in Table 3.

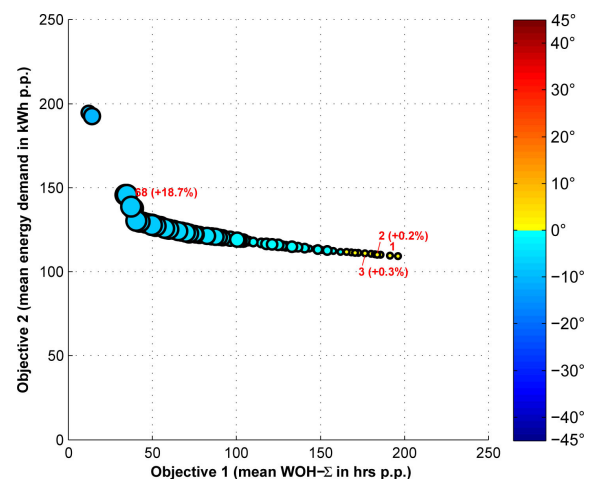


Figure 7: Scatter plot of the mean performance indicator values for all Pareto solutions. The dot size is proportional to  $R$  (smallest  $R = 1.75$ , largest  $R = 2.08$ ), and is not related to the scales on the axes! The three solutions with the smallest  $R$  and the solution with the largest  $R$  are marked with numbers (ascending from small to large). The dot color indicates  $\alpha$  according to the bar on the right.



Table 3: Performance indicators of the three most robust solutions and the least robust solution.

|             | Mean WOH- $\Sigma$<br>[hours/spring] | Mean energy<br>demand<br>[kWh/spring] | R    | $\alpha$<br>[°] |
|-------------|--------------------------------------|---------------------------------------|------|-----------------|
| Solution 1  | 191                                  | 109                                   | 1.75 | 2.5             |
| Solution 2  | 186                                  | 110                                   | 1.75 | 2.3             |
| Solution 3  | 180                                  | 111                                   | 1.75 | 2.2             |
| Solution 68 | 10                                   | 198                                   | 2.08 | -8.0            |

The solution that the DM chose in the example of this section's first paragraph turns out to be unfeasible, because the *mean* number of WOH- $\Sigma$  is higher than the constraint of 200 hours. The solution indicated with number 1 shows the most robust performance with an R of 1.75. Solution 2 and 3 show only small differences of R compared to solution 1 (0.2% and 0.3%). Because the R's of these solutions are so close together, we rank the solutions based on the difference of the  $\alpha$ 's with the preferred  $\alpha$ 's (see also Figure 8). The  $\alpha$ 's of solutions 1, 2 and 3 are respectively 2.5°, 2.3° and 2.2°. The calculated preferred  $\alpha$ 's are 15.5°, 14.7° and 13.8°. Thus, solution 3 shows the smallest difference with its preferred  $\alpha$ : 13.8° - 2.2° = 11.6°. This solution is regarded as the most optimal and robust design, it shows a mean energy demand of 111 kWh in spring and mean WOH- $\Sigma$  of 180 hours. The solution consist of window size: 50% and thermal masses: zone A 5 kg/m<sup>2</sup>, zone B 18 kg/m<sup>2</sup>, zone C and D 100 kg/m<sup>2</sup>, zone E 22 kg/m<sup>2</sup>. The same solution can be found in Figure 5 as the seventh dot from the right.

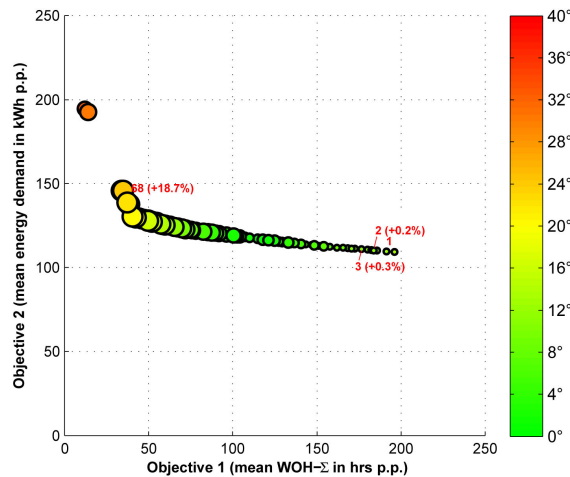


Figure 8: Scatter plot of the mean performance indicator values for all Pareto solutions (see Figure 7). The dot color shows the absolute difference between  $\alpha$  and the preferred  $\alpha$ .

## OPTIMIZATION WITH UNCERTAINTIES DURING THE OPTIMIZATION RUN

In the previous section, the building is optimized for one building user only. The optimization algorithm

did not take uncertainties into account when searching for the Pareto solutions. This might lead to Pareto solutions with a sub-optimal performance (robustness) when the solutions are subjected to uncertainties. In this section, we investigate if the optimization algorithm will find other solutions when uncertainty scenarios are introduced *during* the optimization run (from here on, we call this *optimization under uncertainty*). All designs that are evaluated by the optimization algorithm are simulated with the user behavior scenarios mentioned in the previous section. The objective of the optimization algorithm is to minimize the mean values of the building performance indicators. As mentioned before, we put a constraint on the mean values of the uncertainty scenarios: mean WOH- $\Sigma$  < 200 hours.

The results of the optimization are presented in Figure 9 and Table 4. Shown are the Pareto solutions found after 100 generations with a population size of 10.

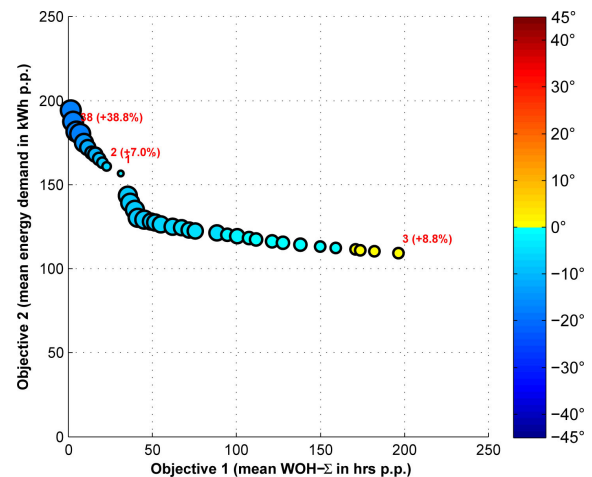


Figure 9: Pareto front of optimization with uncertainties during the optimization run. Shown are the mean performance indicator values of the Pareto solutions. The dot size is proportional to R (smallest R = 1.61, largest R = 2.24), and is not related to the scales on the axes! The three solutions with the smallest R and the solution with the largest R are marked with numbers (ascending from small to large). The dot color indicates  $\alpha$  according to the color bar on the right.

Table 4: Performance indicators of the three most robust solutions and the least robust solution for optimization with uncertainties during the optimization run.

|             | Mean WOH- $\Sigma$<br>[hours/spring] | Mean energy<br>demand<br>[kWh/spring] | R    | $\alpha$<br>[°] |
|-------------|--------------------------------------|---------------------------------------|------|-----------------|
| Solution 1  | 31                                   | 157                                   | 1.61 | -3.1            |
| Solution 2  | 23                                   | 161                                   | 1.73 | -6.7            |
| Solution 3  | 196                                  | 109                                   | 1.76 | 2.2             |
| Solution 38 | 5                                    | 182                                   | 2.24 | -17.3           |

The R of the Pareto solution 1 (R = 1.61) is 7% smaller than the R of the solution 2 (R = 1.73), thus

solution 1 can be regarded as the most robust solution. This solution provides a mean energy demand of 157 kWh and a mean WOH- $\Sigma$  of 31 hours for spring. The solution consists of 25% glazing and the following thermal masses: zone A 5 kg/m<sup>2</sup>, zone B 7 kg/m<sup>2</sup>, zone C and D 5 kg/m<sup>2</sup>, zone E 5 kg/m<sup>2</sup>. The difference in R between solution 2 and 3 is 2%. If the DM finds this difference too small for ranking the solutions, then he can use the preferred  $\alpha$ 's. Solution 2 shows an  $\alpha$  of -6.7° and solution 3 an  $\alpha$  of 1.6°, while the calculated preferred  $\alpha$ 's are -37.0° and 15.7°. This means that solution 3 shows the smallest difference with 13.5° and is preferred over solution 2 (see Figure 10).

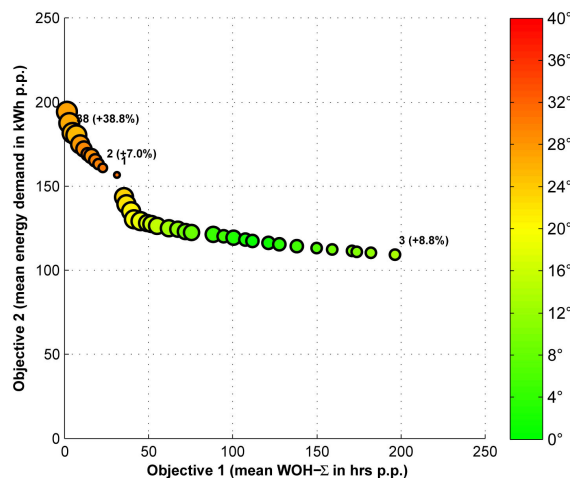


Figure 10: Scatter plot of the mean performance indicator values for all Pareto solutions (see Figure 9). The dot color shows the absolute difference between  $\alpha$  and the preferred  $\alpha$ .

The solutions found when using optimization under uncertainty are more diverse and more uniformly distributed over the Pareto front than the solutions found by the run with uncertainties after the optimization (compare Figure 7 and 9). All solutions found by the latter method are also found by the first method. However, in addition, the first method also explores (Pareto) solutions that were discarded by the optimization run without uncertainties. In this case study, one of these discarded solutions turns out to be one of the most robust solutions (Pareto solution 1 in Figure 9).

## CONCLUSIONS

The proposed selection methodology provides the decision maker (DM) with information about the performance robustness of design solutions. Using this information, the DM is able to select the most robust solution from a set of (Pareto) design solutions. Without the proposed robustness indicator, the DM would typically prefer solutions

on the knee-point of the Pareto front. However, using the robustness indicator, it might turn out that solutions on the end points of the Pareto front are more robust and thus more preferable.

The simulation results of the case study building show that changes in user behavior have a large impact on the building's performance indicators. This stresses the importance of taking uncertainties in user behavior into account during the design process since in many cases the actual user behavior is unknown. We showed that it is possible to take these uncertainties into account during the design optimization process. In combination with the proposed selection methodology, this leads to design solutions with a robust building performance.

The results of this case study show that the method with uncertainties during the optimization is preferred over the method that calculates uncertainties after the optimization run. The first method provides the DM with a more diverse range of solutions. However, this method requires a much higher computational load, since every solution that the optimization algorithm assesses needs to be simulated with all uncertainty scenarios.

In this paper, we chose to use fixed uncertainty scenarios. In the future of this project, we want to use stochastic user models and generate a larger group of random uncertainty scenarios. Furthermore, besides uncertainties in user behavior, we will also incorporate other uncertainties, e.g. uncertainties in climate scenarios.

## ACKNOWLEDGEMENT

This research was carried out under the project number M81.1.08319 in the framework of the Research Program of the Materials innovation institute M2i ([www.m2i.nl](http://www.m2i.nl)).

## REFERENCES

- Andersen (2009) - Occupant behaviour with regard to control of the indoor environment – Ph.D. thesis, Technical University of Denmark.
- Bourgeois, D. (2005) - Detailed occupancy prediction, occupancy-sensing control and advanced behavioural modelling within whole-building energy simulation - Ph.D. thesis, l'Université Laval, Québec.
- Clarke, J.A. (2001) – Energy simulation in building design – second edition, Oxford, Butterworth-Heinemann.
- Coello Coello (2006) - Twenty Years of Evolutionary Multi-Objective Optimization: A Historical View of the Field - IEEE

- Computational Intelligence Magazine, vol. 1, no: 1.
- Deb, K., Meyarivan, T., Pratap, A., Agarwal, S. (2002) - A Fast and Elitist Multiobjective Genetic Algorithm: NSGA-II - IEEE Transactions on Evolutionary Computation, vol. 6, no. 2, pp. 182-197.
- Emmerich, M.T.M., Hopfe, C., Marijt, R., Hensen, J.L.M., Struck, C., Stoelinga, P.A.L. (2008) – Evaluating optimization methodologies for future integration in building performance tools - Proceedings of the 8th Int. Conf. on Adaptive Computing in Design and Manufacture.
- Ferguson, S., Siddiqi, A., Lewis, K., De Weck, O.L. (2007) – Flexible and reconfigurable systems: nomenclature and review – Proceedings IDETC/CIE 2007, USA.
- Haldi (2009) - Towards a unified model of occupants' behaviour and comfort for building energy simulation – Ph.D. thesis, École Polytechnique Fédérale de Lausanne.
- Hoes, P., Hensen, J.L.M., Loomans, M.G.L.C., Vries, B. de, Bourgeois, D. (2009) - User behavior in whole building simulation - Energy and Buildings, 41(3), 295-302.
- Hoes, P., Trcka, M., Hensen, J.L.M., B. Hoekstra Bonnema (2010) – Exploring the optimal thermal mass to investigate the potential of a novel low-energy house concept – Proceedings 10th International Conference for Enhanced Building Operations.
- Hoes, P., Trcka, M., Hensen, J.L.M., B. Hoekstra Bonnema (2011) – Investigating the potential of a novel low-energy house concept with hybrid adaptable thermal storage – Energy Conversion and Management, 52(6), 2442-2447.
- Hopfe, C.J. (2009) – Uncertainty and sensitivity analysis in building performance simulation for decision support and design optimization – Ph.D. thesis, Eindhoven University of Technology.
- Leyten, J.L., Kurvers, S.R. (2006) - Robustness of buildings and HVAC systems as a hypothetical construct explaining differences in building related health and comfort symptoms and complaint rates - Energy and Buildings, 38 (6), 701–707.
- Macdonald, I.A. (2002) - Quantifying the effects of uncertainty in building simulation – Ph.D. thesis, University of Strathclyde.
- Parys (2010) - Implementing realistic occupant behavior in building energy simulations – the effect on the results of an optimization of office buildings - REHVA World Congress, Antalya.
- Tabak (2010) - Methods for the prediction of intermediate activities by office occupants – Building and Environment, 45, 1366-1372.